Transport Properties in Gases at High Temperature and Low Pressure: Comparison of Kinetic Theory with Direct Simulation Monte Carlo

D. Omeiri · D. E. Djafri

Abstract   Expressions for the transport coefficients obtained from the Gross-Jackson and the Chapman–Enskog methods are used to derive explicit relations incorporating the internal energy of the molecules for pure polyatomic gases and for binary mixtures of gases. Various coefficients such as the binary diffusion, thermal conductivity, and the viscosity coefficients and the thermal diffusion factor are calculated and a comparison with the direct simulation Monte Carlo (DSMC) method is carried out. The results show that the contribution of the internal energy is important and cannot be neglected.

Keywords   Direct simulation Monte Carlo · Kinetic theory · Transport coefficients

List of Symbols

b	Impact parameter
c_p^{rot}	Molecular specific heat of rotation, $\text{J} \cdot \text{K}^{-1}$
c_p^{vib}	Molecular specific heat of vibration, $\text{J} \cdot \text{K}^{-1}$
dtm	Time step, s
d_p, d_q	Diameter of molecule p or q, m
D_{pq}	Coefficient of diffusion in a binary gas mixture, $\text{m}^2 \cdot \text{s}^{-1}$
$[D_{pq}]_{N=L}$	Lth-order approximation of D_{pq}, $\text{m}^2 \cdot \text{s}^{-1}$
$D_p^{\text{T}}, D_q^{\text{T}}$	Coefficient of thermal diffusion, $\text{kg} \cdot \text{m}^{-1} \cdot \text{s}^{-1}$
$[D^{\text{T}}]_{N=L}$	Lth-order approximation of D^{T}, $\text{kg} \cdot \text{m}^{-1} \cdot \text{s}^{-1}$

D. Omeiri
Laboratoire de Physico-Chimie des Surfaces, Université de Skikda, Skikda, Algeria

D. E. Djafri (✉)
Laboratoire de Physique des Lasers, Université d' Annaba, B.P. 12, Annaba 23000, Algeria
e-mail: dedjafri@yahoo.fr

D_{pp}	Coefficient of self diffusion, $m^2 \cdot s^{-1}$
$\boldsymbol{g}_{pq}$	Relative velocity vector of the colliding molecules, $m \cdot s^{-1}$
I_{ij}^{kl}	Differential collision cross section, m^2
$(\boldsymbol{j_p})_{N=3}$	Flux vector, $kg \cdot m^{-2} \cdot s^{-1}$
k	Boltzmann constant, $k = 1.38 \times 10^{-23}\ J \cdot K^{-1}$
Kn	Knudsen number
K_{tot}	Total coefficient of thermal conductivity, $W \cdot m^{-1} \cdot K^{-1}$
K_{trans}	Translational thermal conductivity, $W \cdot m^{-1} \cdot K^{-1}$
K_{rot}	Rotational thermal conductivity, $W \cdot m^{-1} \cdot K^{-1}$
K_{vib}	Vibrational thermal conductivity, $W \cdot m^{-1} \cdot K^{-1}$
k_T	Thermal diffusion ratio
m_p, m_q	Mass of molecule p or q, kg
m_{pq}	Reduced mass of molecules p and q, kg
N	Total number of molecules
n	Total number density, m^{-3}
n_p, n_q	Number density of species p and q, m^{-3}
P	Pressure, $N \cdot m^{-2}$
$\boldsymbol{q}$	Heat flux vector, $W \cdot m^{-2}$
Q	Total collision cross section, m^2
r	Intermolecular separation, m
$\boldsymbol{r}$	Position vector, m
T	Temperature, K
$\boldsymbol{v}_p$	Diffusion velocity of species p, $m \cdot s^{-1}$
X_p, X_q	Mole fraction of species p or q
Z_p^{rot}	Rotational relaxation collision number for molecule p
Z_p^{vib}	Vibrational relaxation collision number for molecule p
α_{pq}	Parameter for VSS potential
α_T	Thermal diffusion factor
Γ	Euler's Gamma function
γ	Dimensionless relative velocity vector
λ	Mean free path, m
$\varphi(r)$	Intermolecular potential
φ	Azimuthal angle, radian
μ	Shear viscosity, $kg \cdot m^{-1} \cdot s^{-1}$
ν	Collision rate, s^{-1}
Ω	Solid angle of diffusion, steradian
$\boldsymbol{\Omega}_{pq}^{(l,s)}$	Collision integral
ρ	Density, $kg \cdot m^{-3}$
ω_p, ω_q	Temperature exponent of the viscosity coefficient for VSS or VHS potentials
χ	Deflection angle, radian
θ_r	Characteristic temperature of rotational mode, K
θ_v	Characteristic temperature of vibrational mode, K
τ	Viscosity stress tensor, $N \cdot m^{-2}$

Subscripts

int	Internal modes
p,q	Particular molecular species
ref	Reference value
trans	Translational modes

Subscripts and Superscripts

rot	Rotational modes
vib	Vibrational modes

1 Introduction

The development of a variety of devices such as low-pressure chemical vapor deposition (CVD) reactors and micro-electromechanical systems (MEMS) has led researchers to concentrate on the study of transport properties in the non-continuum regime ($Kn > 0.01$). In this regime, we distinguish two cases: the first case, called the low-pressure case characterized by a large mean free path of the molecules, and the second case due to a micro-length scale. The conventional continuum methods used for analyzing transport problems are based on the fact that transport properties such as viscous dissipation or thermal conduction are evaluated from bulk flow quantities such as temperature or velocity. This leads to inaccuracies when the characteristic length of the flow gradients is comparable to the molecules' mean free path. The direct simulation Monte Carlo (DSMC) method has proven to be very effective for solving problems with a high Knudsen number.

Now, on a larger scale, the study of the physicochemical phenomena appearing during spacecraft re-entry is based on solving the Navier–Stokes equations, coupled with kinetic and vibrational relaxation equations. The theoretical determination of the transport coefficients appearing in these equations is a complex problem. The analysis of the transport properties in pure or mixed gas flows in the collisional regime is usually carried out following three methods, all based on solving the Boltzmann equation: the method of moments [1,2], the Gross Jackson method [3], and the Chapman–Enskog method (CE) [4]. The first two methods may be extended to transitional regimes, but in the collisional regime, the CE method seems to be more appropriate. In this case, the molecular velocity distribution function is expanded in series in terms of the Knudsen number, which is the ratio of the elastic collision characteristic time to the reference flow time. In the weak nonequilibrium (WNE) case and for elastic collisions [5,6], Chapman–Enskog methods [4] give results that are in good agreement with experiment. The extension of these methods to gases whose structure is more complex is, however, more difficult because of the inelastic collisions, particularly when nonequilibrium conditions prevail [7]. Collisions integrals associated with internal energy exchanges are required for the evaluation of transport properties of polyatomic species mixtures. In our work, we are mostly interested in the dilute-gas limit, regime for which the Chapman–Enskog method is valid.

We will give explicit relations for the transport coefficients that take into account the internal energy of the molecules. These coefficients are functions of collision inte-

grals that depend on the molecular collision dynamics. Using the Mason and Monchick approximations [8,9] and, assuming the harmonic oscillator model for diatomic molecules, expressions for the transport coefficients are given in explicit form.

The binary diffusion coefficient and the thermal diffusion factor derived from the Gross–Jackson method [10] with approximations of Monchick et al. [11] are calculated for the variable soft sphere (VSS) molecular potential model of Koura and Matsumoto [12,13] for a binary mixture of gases. These two coefficients are also calculated with the DSMC method with the VSS molecular potential model implemented in it: the binary diffusion coefficient is evaluated through a simulation where we have two reservoirs of gases, i.e., two concentration gradients at uniform pressure and temperature; the thermal diffusion factor is evaluated from a simulation in a binary mixture of gases at uniform pressure sustaining a temperature gradient. The influence of the vibrational energy on the thermal diffusion factor is also examined.

The thermal conductivity and the viscosity coefficients are evaluated for pure polyatomic gases with the Chapman–Enskog method. These coefficients are also calculated with the DSMC method through various simulations of a uniform shear flow or Couette flow. In both methods, the VSS molecular potential model was used.

2 Transport Coefficients

2.1 Boltzmann Equation

Let $f_{ip} = f(v_p, E_{ip}, r, t)$ be the distribution function where

- ip designates the internal state of molecule p,
- v_p is its velocity,
- E_{ip} is its internal energy,
- r is its position at time t

The Boltzmann equation for molecule p in the absence of external forces is

$$\frac{\partial f_{ip}}{\partial t} + v_p \frac{\partial f_{ip}}{\partial r} = \sum_q J_{pq}\left(f_{ip}, f_{jq}\right)$$

$$= \sum_q \sum_{jkl} \iiint \left(f'_{kp} f'_{lq} - f_{ip} f_{jq}\right) g_{pq} I^{kl}_{ij} \sin\chi \, d\chi \, d\varphi \, dv_q \quad (1)$$

where ip and jq represent the internal state of molecules p and q before collision and kp and lq their state after collision; if $g_{pq} = v_p - v_q$ is the relative velocity of molecules p and q before collision and $g'_{pq} = v'_p - v'_q$ their relative velocity after collision, then, χ and φ are, respectively, the polar and azimuthal angles which describe the orientation of g'_{pq} relative to g_{pq}; $f'_{kp} = f(v'_p, E_{kp}, r, t)$; $f'_{lq} = f\left(v'_q, E_{lq}, r, t\right)$; $f_{jq} = f\left(v_q, E_{jq}, r, t\right)$; and I^{kl}_{ij} is the differential collision cross section.

2.2 Diffusion in a Binary Mixture of Gases

Using the method of Gross–Jackson to solve Eq. 1, we get the formal expression of the flux,

$$(j_p)_{N=3} = -\frac{n^2}{\rho} m_p m_q \left[D_{pq} \right]_{N=3} \left(\frac{\partial}{\partial \boldsymbol{r}} \left(\frac{n_p}{n} \right) + \left(\frac{n_p}{n} - \frac{n_p m_p}{\rho} \right) \frac{\partial \ln(P)}{\partial \boldsymbol{r}} \right)$$
$$- \left[D^{\mathrm{T}} \right]_{N=3} \frac{\partial \ln(T)}{\partial \boldsymbol{r}} \tag{2}$$

where n is the number of particles per unit volume, m_p and m_q are the masses of molecules p and q, respectively, and ρ is the density of the mixture.

$[D_{pq}]_{N=3}$ is the third-order coefficient of binary diffusion in the Gross–Jackson approximation and is written as a ratio of determinants $|4 \times 4|/|5 \times 5|$ [10]:

$$[D_{12}]_{N=3} = \frac{kT}{nm_1} \begin{bmatrix} \Delta^{10,10} & \Delta^{01,10} \\ \Delta^{10,01} & \Delta^{01,01} \end{bmatrix} \Bigg/ \begin{bmatrix} \Delta^{00,00} & \Delta^{10,00} & \Delta^{01,00} \\ \Delta^{00,10} & \Delta^{10,10} & \Delta^{01,10} \\ \Delta^{00,01} & \Delta^{10,01} & \Delta^{01,01} \end{bmatrix} \tag{3}$$

$\left[D^{\mathrm{T}} \right]_{N=3}$ is the third-order coefficient of thermal diffusion and is written as a ratio of determinants $|5 \times 5|/|5 \times 5|$ [10]:

$$\left[D^{\mathrm{T}} \right]_{N=3} = \frac{\rho_1 \rho_2}{\rho kT X_2} \begin{bmatrix} 0 & M^{10,00} & M^{01,00} \\ X_1 & & \\ X_2 & M^{10,10} & M^{01,10} \\ X_1 & & \\ X_2 & M^{10,01} & M^{01,01} \end{bmatrix} \Bigg/ \begin{bmatrix} M^{00,00} & M^{10,00} & M^{01,00} \\ M^{00,10} & M^{10,10} & M^{01,10} \\ M^{00,01} & M^{10,01} & M^{01,01} \end{bmatrix} \tag{4}$$

X_1 and X_2 are the mole fractions of species 1 and species 2, respectively. Monchick et al. [9] found it to be a $|7 \times 7|/|6 \times 6|$ ratio.

The elements of these determinants are complicated functions of the collision integrals and can be found in Ref. [10]. When there are no inelastic collisions, these coefficients reduce to the second Chapman–Enskog approximation to the binary and thermal diffusion coefficients [4].

The thermal diffusion factor α_{T} is defined by the following expression:

$$\alpha_{\mathrm{T}} = \frac{\rho}{\rho_1 \rho_2} \left[D^{\mathrm{T}} \right]_{N=3} \Bigg/ [D_{12}]_{N=1} \tag{5}$$

$[D_{12}]_{N=1}$ corresponds to the first-order approximation to the coefficient of diffusion in a binary mixture of gases in the Chapman–Enskog expansion, ρ_1, ρ_2, and ρ are the densities of species 1, species 2, and of the mixture, respectively. α_{T} can be put in the form

$$\alpha_{\mathrm{T}} = \alpha_{\mathrm{trans}} + \alpha_{\mathrm{int}} \tag{6}$$

α_{trans} is the contribution of the translational energy and α_{int} that of the internal energy (rotation and vibration).

The thermal diffusion ratio is given by

$$k_{\text{T}} = X_1 X_2 \alpha_{\text{T}} \tag{7}$$

The contribution of the internal energy to the binary diffusion coefficient is small [11], so, $[D_{12}]_{N=3}$ in the Gross–Jackson expansion, corresponds to $[D_{12}]_{N=2}$ in the Chapman–Enskog expansion defined in [4] where only translational energy exchanges are taken into account in calculating this coefficient.

2.3 Thermal Conductivity and Viscosity in Pure Polyatomic Gases in Weak Nonequilibrium (WNE)

Using the Chapman–Enskog method in the WNE case we get the expression of the heat flux $\boldsymbol{q}$,

$$\boldsymbol{q} = \boldsymbol{q}_{\text{trans}} + \boldsymbol{q}_{\text{rot}} + \boldsymbol{q}_{\text{vib}} = -K_{\text{tot}} \frac{\partial T}{\partial \boldsymbol{r}} \tag{8}$$

where K_{tot}, the coefficient of thermal conductivity, is also written as a sum of translational, rotational, and vibrational contributions:

$$K_{\text{tot}} = K_{\text{trans}} + K_{\text{rot}} + K_{\text{vib}} \tag{9}$$

Here, we have a single chemical species. The explicit formal expressions for K_{trans}, K_{rot}, and K_{vib} are given in [8,9] by

$$K_{\text{trans}} = -\frac{15}{4} \mu_p \frac{k}{m_p} \left(1 - \frac{10}{3\pi k} \left(\frac{c_p^{\text{rot}}}{Z_p^{\text{rot}}} + \frac{c_p^{\text{vib}}}{Z_p^{\text{vib}}} \right) \right) + \frac{5}{\pi} n_p D_{pp} \left(\frac{c_p^{\text{rot}}}{Z_p^{\text{rot}}} + \frac{c_p^{\text{vib}}}{Z_p^{\text{vib}}} \right) \tag{10}$$

$$K_{\text{rot}} = n_p D_{pp} c_p^{\text{rot}} \left(1 - \frac{2}{\pi} \frac{\rho D_{pp}}{\mu_p} \frac{1}{Z_p^{\text{rot}}} \right) + \frac{5}{\pi} n_p D_{pp} \frac{c_p^{\text{rot}}}{Z_p^{\text{rot}}} \tag{11}$$

$$K_{\text{vib}} = n_p D_{pp} c_p^{\text{vib}} \left(1 - \frac{2}{\pi} \frac{\rho D_{pp}}{\mu_p} \frac{1}{Z_p^{\text{vib}}} \right) + \frac{5}{\pi} n_p D_{pp} \frac{c_p^{\text{vib}}}{Z_p^{\text{vib}}} \tag{12}$$

In these expressions, c_p^{rot} is the molecular specific heat of rotation and is equal to k for a diatomic gas and c_p^{vib} is the molecular specific heat of vibration. Its expression for an harmonic oscillator is

$$c_p^{\text{vib}} = k \left(\frac{\theta_{\text{v}}/2T}{\sinh(\theta_{\text{v}}/2T)} \right)^2 \tag{13}$$

where θ_{v} is the characteristic temperature of vibration.

D_{pp} is the coefficient of self diffusion:

$$D_{pp} = \frac{3kT}{8nm_p \boldsymbol{\Omega}_{pp}^{(1,1)}} \tag{14}$$

and μ_p is the dynamic viscosity given in [4]:

$$\mu_p = \frac{5}{8} \frac{kT}{\boldsymbol{\Omega}_{pp}^{(2,2)}} \tag{15}$$

The expressions of the collision integrals $\boldsymbol{\Omega}_{pp}^{(1,1)}$ and $\boldsymbol{\Omega}_{pp}^{(2,2)}$ are given in the appendix. The expression of the rotational relaxation collision number Z_p^{rot} is given by Parker's formula [14,15],

$$Z_p^{\text{rot}} = Z_\infty^{\text{rot}} \left[1 + \frac{\pi^{3/2}}{2} \left(\frac{\theta_{\text{r}}}{T} \right)^{1/2} + \left(\frac{\pi^2}{4} + \pi \right) \left(\frac{\theta_{\text{r}}}{T} \right) \right]^{-1} \tag{16}$$

where Z_∞^{rot} is the limiting value of Z_p^{rot} at high temperatures. For our theoretical calculations for nitrogen, $Z_\infty^{\text{rot}} = 15.7$ and $\theta_{\text{r}} = 80.0$ K.

The vibrational relaxation collision number Z_p^{vib} is evaluated from the experimental data found in [16,17]

$$Z_p^{\text{vib}} = \frac{C_1}{T^\omega} \exp \left(C_2 T^{-\frac{1}{3}} \right) \tag{17}$$

where C_1 and C_2 are constants depending on the nature of the gas under consideration; ω is the temperature exponent of the coefficient of viscosity: $\mu \propto T^\omega$.

3 DSMC Method

3.1 Description

The DSMC method, pioneered by Bird [17], is used to obtain the density, pressure, velocity, and the translational, rotational, and vibrational temperature fields in the simulated physical space. As a result, the DSMC is accurate for problems in which the degree of rarefaction in flow fields is high or when the characteristic length is small. The degree of rarefaction is characterized by the Knudsen number, which is the ratio of the mean free path λ to a typical dimension L of the flow field ($Kn = \lambda/L$). The Kn domain is often divided into four flow regimes. When $Kn < 0.01$, the usual continuum assumption is valid, and the Navier–Stokes equations are applicable in their common form. When $0.01 < Kn < 0.1$, we are in the slip-flow regime, and the Navier–Stokes equations are used with the usual no-slip wall boundary condition replaced with a slip-flow boundary condition. When $0.1 < Kn < 10$, we are in the transition regime, and the Navier–Stokes equations are no longer valid. DSMC is an effective tool for

studying the fluid effects in the flow field. When $Kn > 10$, we are in the free molecular regime, and the flow is sufficiently rarefied to neglect molecular collisions. The collisionless Boltzmann equation is therefore applicable.

In the DSMC method, a real gas is simulated by thousands or millions of molecules. The positions, velocities, and initial states of these simulated particles are stored and modified in time as they are moving, colliding among themselves, and interacting with boundaries in the simulated physical space. Each simulated particle represents a very large number of physical molecules. In this method, the number of molecular trajectories and molecular collisions that must be calculated is substantially reduced. Furthermore, the DSMC method uncouples the analysis of the molecular motion from that of the molecular collisions by use of a time step dtm smaller than the real physical collision time ($dtm < 1/\nu$ where ν is the collision rate). The DSMC method applied to low-pressure fluid flow simulation is intuitively attractive, because it is valid for all flow regimes. Generally, in the DSMC framework, high-velocity flows are much easier to study than low-velocity flows because of the statistical fluctuations [17]. In DSMC, the computational time step must be less than the mean collision time. Another condition that must be satisfied during a DSMC procedure is that the smallest size of the computational cells must not be greater than one-third of the mean-free path. In addition, the importance of statistical fluctuations caused by small perturbations, increases as the flow velocity gets smaller. The statistical fluctuations decrease with the square root of the sample size.

3.2 Numerical Experiment with the DSMC Method

3.2.1 Review of the Theory

The mean diffusion velocity $\boldsymbol{V}_i$ of species i in the medium is given by

$$\boldsymbol{V}_i = \left(\frac{n^2}{n_i \rho}\right) \sum_j m_j D_{ij} \boldsymbol{d}_j - \frac{D_i^{\mathrm{T}}}{n_i m_i} \frac{\partial \ln(T)}{\partial \boldsymbol{r}} \tag{18}$$

The flux $\boldsymbol{j}_i$ of species i is

$$\boldsymbol{j}_i = n_i m_i \boldsymbol{V}_i = \frac{n^2}{\rho} \sum_{j=1}^{\nu} m_i m_j D_{ij} \boldsymbol{d}_j - D_i^{\mathrm{T}} \frac{\partial \ln(T)}{\partial \boldsymbol{r}} \tag{19}$$

with

$$\boldsymbol{d}_j = \frac{\partial}{\partial \boldsymbol{r}} \left(\frac{n_j}{n}\right) + \left(\frac{n_j}{n} - \frac{n_j m_j}{\rho}\right) \frac{\partial \ln(P)}{\partial \boldsymbol{r}} + \frac{n_j m_j}{P \rho} \left(\frac{\rho}{m_j} \boldsymbol{X}_j - \sum_{k=1}^{\nu} n_k \boldsymbol{X}_k\right) \tag{20}$$

$\boldsymbol{X}_k$ represent all external forces acting on the molecules.

The ν Eq. 19 for each one of the species can be replaced by $\nu - 1$ independent relations

$$\sum_{\substack{j=1 \\ j \neq i}}^{v} \frac{n_i n_j}{n^2 D_{ij}} \left(V_j - V_i \right) = d_i - \frac{\partial \ln(T)}{\partial r} \sum_{\substack{j=1 \\ j \neq i}}^{v} \frac{n_i n_j}{n^2 D_{ij}} \left(\frac{D_j^{\mathrm{T}}}{n_j m_j} - \frac{D_i^{\mathrm{T}}}{n_i m_i} \right) \quad (21)$$

For a binary mixture, Eq. 19 can be written as

$$j_1 = n_1 m_1 V_1 = \frac{n^2}{\rho} m_1 m_2 D_{12} d_1 - D_1^{\mathrm{T}} \frac{\partial \ln(T)}{\partial r} \quad (22)$$

Since $d_1 = -d_2$ and $j_1 = -j_2$, we have $D_{12} = D_{21}$ and $D_1^{\mathrm{T}} = -D_2^{\mathrm{T}}$, and Eq. 21 can be put into the form,

$$V_1 - V_2 = -\frac{n^2}{n_1 n_2} D_{12} \left(d_1 + k_{\mathrm{T}} \frac{\partial \ln(T)}{\partial r} \right) \quad (23)$$

in the absence of external forces, Eq. 23 becomes

$$V_1 - V_2 = -\frac{n^2}{n_1 n_2} D_{12} \left(\frac{\partial}{\partial r} \left(\frac{n_1}{n} \right) + \left(\frac{n_1}{n} - \frac{n_1 m_1}{\rho} \right) \frac{\partial \ln(P)}{\partial r} + k_{\mathrm{T}} \frac{\partial \ln(T)}{\partial r} \right) \quad (24)$$

where k_{T} is the thermal diffusion ratio defined by

$$k_{\mathrm{T}} = \frac{\rho}{n^2 m_1 m_2} \frac{D_1^{\mathrm{T}}}{D_{12}} \quad (25)$$

and α_{T} is the thermal diffusion factor related to k_{T} by

$$\alpha_{\mathrm{T}} = \frac{n^2}{n_1 n_2} k_{\mathrm{T}} \quad (26)$$

3.2.2 Applications

The first application concerns a binary mixture of gases. For our calculations, we used the DS2G code of Bird, taking into account the rotational and vibrational energies as well as the chemical reactions. For very small temperature and pressure gradients, Eq. 24 reduces to

$$V_1 - V_2 = -\frac{n^2}{n_1 n_2} D_{12} \frac{\partial}{\partial r} \left(\frac{n_1}{n} \right) \quad (27)$$

For a one-dimensional flow, the binary diffusion coefficient is simply

$$D_{12} = - (V_1 - V_2) \frac{n_1}{n} \frac{n_2}{n} \frac{\Delta y}{\Delta (n_1/n)} \quad (28)$$

This equation is used to determine the values of the binary diffusion coefficient from simulation.

For the calculation of the diffusion coefficient D_{12} in a binary mixture of gases from simulation, we have two reservoirs of gases, i.e., two concentration gradients, at uniform pressure and temperature as illustrated in Fig. 1. The flow field is filled with an argon reservoir at the inner boundary ($y = 0$) and with a nitrogen reservoir at the outer boundary ($y = 1$ m). In order to keep the local Knudsen number within the range of values for which the Chapman–Enskog theory is applicable, the number density in each reservoir is set to 2.8×10^{20} m^{-3}. The molecular properties of the VSS model used for argon and nitrogen are listed in Table 1.

The time step dtm is the time over which the molecular motion is uncoupled from the intermolecular collisions. It should be small in comparison with the local mean collision time. It was set to 0.5×10^{-6} s. The number of cells in the y-direction was set to 200.

In the case of a Fourier flow, the relative diffusion velocities and the pressure diffusion term are negligible, so, Eq. 24 reduces to

$$\left(\frac{\partial}{\partial \boldsymbol{r}} \left(\frac{n_1}{n} \right) + k_{\mathrm{T}} \frac{\partial \ln(T)}{\partial \boldsymbol{r}} \right) = 0 \tag{29}$$

Reservoir N$_2$

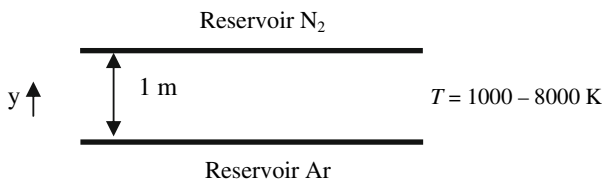$y \uparrow$ 1 m $T = 1000 - 8000$ K

Reservoir Ar

Fig. 1 Experimental arrangement for the binary diffusion coefficient

Table 1 Physicochemical properties of argon and nitrogen used in the DS2G code [17]

Parameters	Units	Argon	Nitrogen
d_{ref}	m	4.11×10^{-10}	4.11×10^{-10}
T_{ref}	K	273	273
ω	–	0.81	0.74
α	–	1.4	1.36
m	kg	66.3×10^{-27}	46.5×10^{-27}
Z_{rot}	–	–	5
θ_{v}	K	–	3395
C_1	–	–	9.1
C_2	–	–	220

Using Eq. 26, and the fact that $n = n_1 + n_2$, then, a straightforward integration of Eq. 29 yields

$$\ln(n_1/n_2) = -\alpha_T \ln(T) + C \tag{30}$$

where C is a constant. Therefore, a plot of $\ln(n_1/n_2)$ versus $\ln(T)$ should be a straight line, and from it we can determine α_T.

The thermal diffusion factor α_T is calculated from simulations in a binary mixture of gases at uniform pressure and concentration sustaining a temperature gradient in the $+y$-direction as illustrated in Fig. 2. The inner boundary (at $y = 0$) is a diffusely reflecting surface at 300 K, and the outer surface (at $y = 1$ m) is a stream boundary of a mixture of equal parts ($N_1 = N_2$) of argon and nitrogen at a temperature T ranging from 1000 K to 8000 K and a total number density of 1×10^{20} molecules per cubic meter. The number of cells was set to 200, and the time step set to 0.3×10^{-5} s.

The second application concerns nitrogen. The viscosity and the thermal conductivity coefficients of this gas are determined through a simulation of a uniform shear flow, i.e., a plane Couette flow as shown in Fig. 3. We used the DSMC1 code of Bird [17] in which we have implemented the vibrational and chemical reactions (dissociation of N_2). The inner boundary ($y = 0$) is a diffusely reflecting surface and is at rest while the outer boundary ($y = 1$ m), a diffusely reflecting surface at the same temperature, moves with a finite velocity in the $+x$-direction. The VSS potential model combined with the Borgnakke–Larsen method [18] was used. The time step was set to 3×10^{-6} s and the number of cells in the y-direction was set to 200. The number density of the nitrogen is set to 10^{20} m^{-3}, and, both surfaces and the gas are at the same temperature T. For Figs. 4 and 5, calculations were performed at $T = 273$ K. For Figs. 9 and 10, the calculations were performed at T ranging from 1000 K to 8000 K.

We made various simulations for different Knudsen numbers. Figures 4 and 5 show the velocity slip and temperature slip profiles. These are of the order of $\lambda \frac{\partial V}{\partial y}$ and $\lambda \frac{\partial T}{\partial y}$, respectively, in agreement with previously published work [17]; λ is the mean free path.

The equations that we used for the determination of the values of the thermal conductivity and the viscosity coefficients from simulation are the following
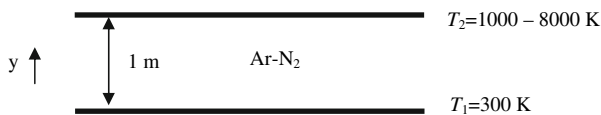

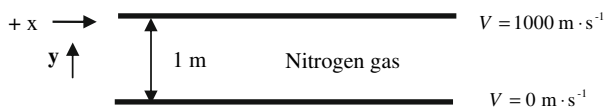**Fig. 2** Experimental arrangement for the thermal diffusion factor

Fig. 3 Figure illustrating the plane Couette flow
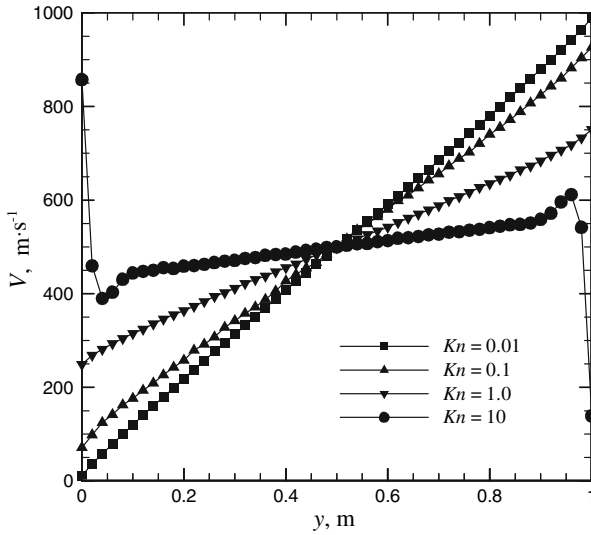
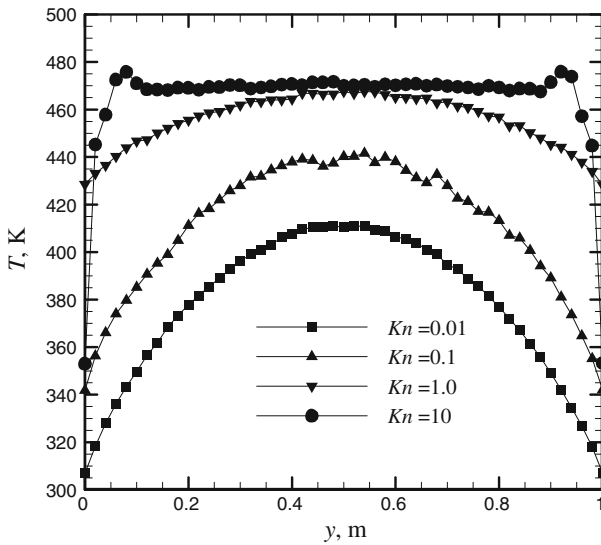**Fig. 4** Velocity slip profiles for nitrogen in a Couette flow

Fig. 5 Temperature slip profiles for nitrogen in a Couette flow

$$K_{\text{tot}} = q \left(\Delta y / \Delta T \right) \tag{31}$$

and

$$\mu = \tau \left(\Delta y / \Delta V \right) \tag{32}$$

4 Results and Discussion

The theoretical results correspond to calculations of transport properties from the expressions derived with the Gross–Jackson and Chapman–Enskog methods and incorporating the internal energy of the molecules of the gas. Simulation is a numerical experiment carried out, in our case, with the DSMC method to evaluate these coefficients. This Monte Carlo technique is applicable for any Knudsen number.

The transport coefficients are functions of collision integrals that depend on the molecular collision dynamics. We have calculated analytically these integrals for the VSS intermolecular potential model with the help of Mathematica software. The computing times were very short, and the analytical expressions that we have obtained are given in the appendix. In this article, we have applied the theory to an Ar–N$_2$ mixture and to pure nitrogen.

- Figure 6 shows that the plot of $\ln(n_1/n_2)$ versus $\ln(T)$ is indeed a straight line, indicating that the approximations made in deriving Eq. 30 are reasonable.
- Figure 7 shows the values of the binary diffusion coefficient D_{12} from simulation and from theory as a function of temperature for a 50 % argon and 50 % nitrogen mixture. We see that the results are in good agreement. The discrepancy between the two models is small at low temperature (less than 3 %) but increases with temperature and reaches 6 % at 8000 K.
- The plot of the thermal diffusion factor α_T as a function of temperature for a 50 % argon and 50 % nitrogen mixture is shown in Fig. 8. It is seen that the results are in good agreement at low temperature (up to 5000 K) and that there are important discrepancies between the two models at higher temperatures. We note that the vibration energy contribution is negligible at low temperature (up to 5000 K) but
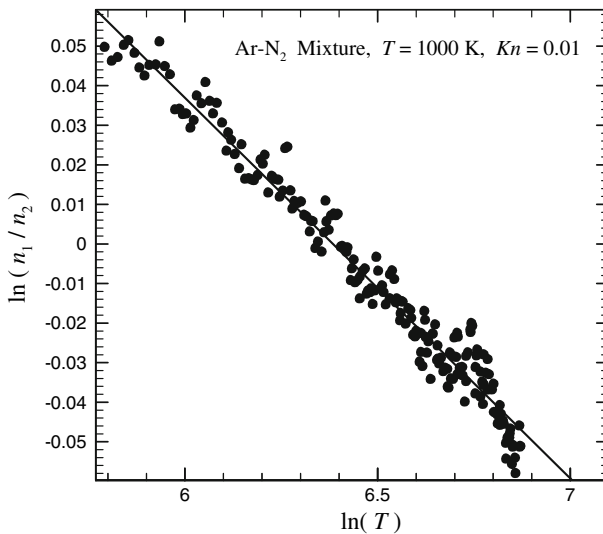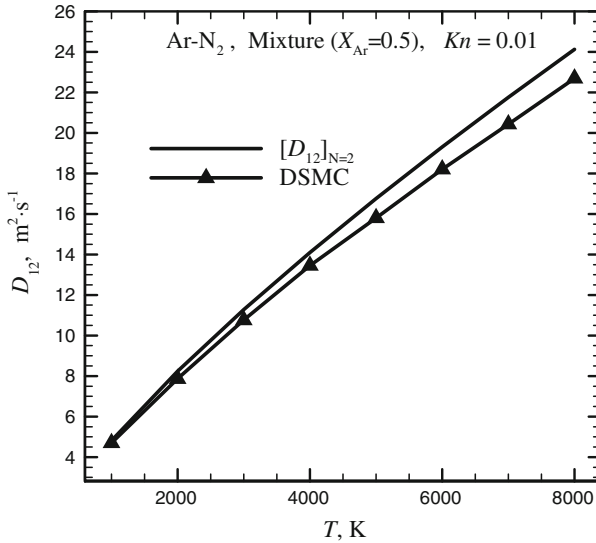

Fig. 6 Plot for the determination of α_T

Fig. 7 Binary diffusion coefficient for an Ar–N$_2$ mixture
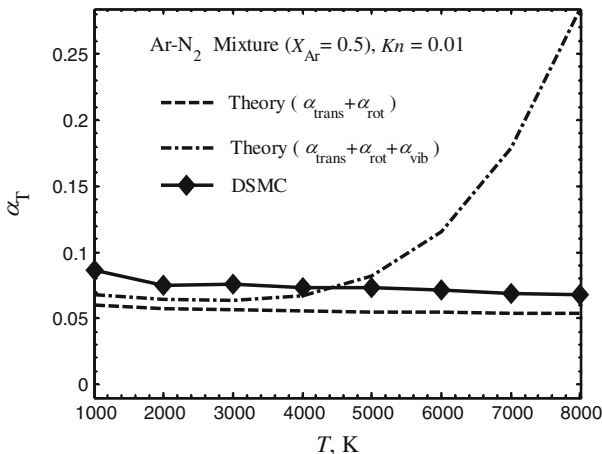

Fig. 8 Thermal diffusion factor α_T for an Ar–N$_2$ mixture

dominates at high temperature. These results indicate that the weak nonequilibrium model (WNE) overestimates the contribution of the vibrational energy.

- In Fig. 9, we have plotted the theoretical values of K_{trans}, $K_{trans} + K_{rot}$, and $K_{tot} = K_{trans} + K_{rot} + K_{vib}$, and the DSMC values of K_{tot} as a function of temperature for nitrogen. We note that the discrepancies between the theoretical and DSMC results are small. This figure shows that the contribution of the vibrational energy to the thermal conductivity is not negligible as has been shown in [19] though a different approach was used: rigid-rotor classical trajectory calculation with inclusion of a correction for vibration.
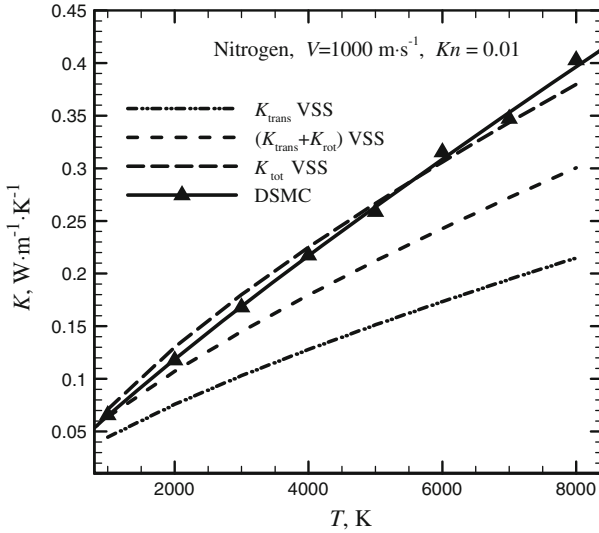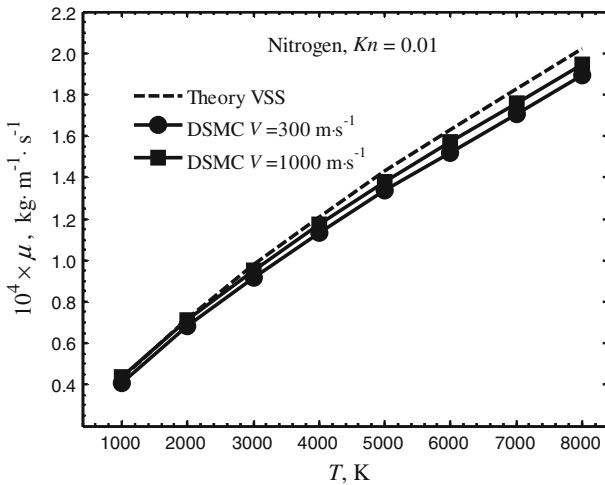
Fig. 9 Thermal conductivity of N_2

Fig. 10 Viscosity coefficient of N_2

- The viscosity coefficient of nitrogen as a function of temperature is plotted in Fig. 10. We see that there is good agreement between the theoretical and DSMC results for both velocities ($V = 300 \, \text{m} \cdot \text{s}^{-1}$ and $V = 1000 \, \text{m} \cdot \text{s}^{-1}$).

5 Conclusion

In this work, starting with the expressions for various transport coefficients obtained from the generalized Gross–Jackson and Chapman–Enskog methods, we have derived

formal expressions for these coefficients that take into account the internal energy of the molecules for pure polyatomic gases and for binary mixtures of gases. Assuming a weak nonequilibrium model (one-temperature model), we have found that for the thermal diffusion factor of a binary mixture of gases, vibrational energy exchanges play an important role at high temperature. At very high temperature, the Gross–Jackson kinetic model overestimates the contribution of the vibrational energy to this coefficient, suggesting that when strong nonequilibrium conditions prevail, a multi-temperature formalism [20] should be used. For the thermal conductivity coefficient of pure polyatomic gases, the contribution from rotation is almost constant and is of the order of 10 % at low and high temperatures, whereas vibration is negligible at low temperature but dominates at high temperature. All this indicates that the internal energy represents an important part and cannot be neglected. Thus, to check the validity of the theory against the DSMC method, we compared the results from these two methods and we have shown that the contribution of the internal degrees of freedom (rotation and vibration) to the thermal conductivity as calculated by the theoretical model is in good agreement with DSMC results.

Appendix

A1 Collision Models

A1.1 Hard-Sphere (HS) Collision Model

The differential cross section $I d\Omega$ for the collision specified by the impact parameter b and ε is defined by $I d\Omega = b db d\varepsilon$, where $d\Omega = \sin \chi d\chi d\varepsilon$ is the element of solid angle and $I = (b/\sin \chi)|db/d\chi|$. The total collision cross section Q is

$$Q = \int_0^{4\pi} I d\Omega = 2\pi \int_0^{\pi} I \sin \chi d\chi \qquad (33)$$

Let us consider a collision between a molecule of species p and one of species q whose effective diameters are d_p and d_q, respectively. The collision becomes effective at a distance $d_{pq} = \frac{1}{2}(d_p + d_q)$. The impact parameter b is related to the deflection angle χ by the expression,

$$b = d_{pq} \sin(\theta_m) = d_{pq} \cos(\chi/2) \qquad (34)$$

θ_m is defined as the value of θ for which r, the intermolecular separation, has a minimum value. This minimum value, r_m, is the distance of closest approach and will be defined shortly. From [16], the angle χ is related to the angle θ_m by the relation,

$$\chi = \pi - 2\theta_m$$

The differential collision cross section is $I = \frac{1}{4}d_{pq}^2$ and $Q = \pi d_{pq}^2$.

A1.2 Variable Hard-Sphere (VHS) Collision Model

This model, developed by Bird [21], uses cross sections that are functions of the relative velocity, but with a hard sphere (HS) scattering angle. We still have $Q = \pi d_{pq}^2$ with

$$d_{pq} = d_{\mathrm{ref}\,pq} \left[\frac{\left(2kT_{\mathrm{ref}} / \left(m_{pq} g_{pq}^2 \right) \right)^{\omega_{pq} - \frac{1}{2}}}{\Gamma(5/2 - \omega_{pq})} \right]^{\frac{1}{2}}$$ (35)

where

$$d_{\mathrm{ref}\,pq} = \frac{1}{2} \left(d_{\mathrm{ref}\,p} + d_{\mathrm{ref}\,q} \right)$$ (36)

Γ is Euler's Gamma function; $d_{\mathrm{ref}\,p}$ and $d_{\mathrm{ref}\,q}$ are the diameters of molecules p and q at temperature $T_{\mathrm{ref}} = 273$ K, and ω_{pq} is the exponent of the temperature in the viscosity coefficient. The value of d_{pq} in the VHS case is adjusted in such a way so as to make the viscosity coefficient proportional to $T^{\omega_{pq}}$ ($\omega_{pq} = 0.5$ for a hard sphere gas and $=1$ for a Maxwell gas). As in the HS model, the scattering angle χ is given by

$$\chi = 2\cos^{-1}\left(b/d_{pq} \right)$$ (37)

A1.3 Variable Soft-Sphere (VSS) Collision Model

The VSS model, developed by Koura and Matsumoto [12,13], is a generalization of the VHS model in which the diameter varies in the same way as in the VHS model, but with a deflection angle χ given by

$$\chi = 2\cos^{-1}\left[\left(b/d_{pq} \right)^{1/\alpha_{pq}} \right]$$ (38)

The parameter α_{pq} is used to characterize the anisotropy of the scattering angle. It is set to 1 if the VHS model is used, and it is set to the appropriate value of the Schmidt number of the gas if the VSS model is used.

A2 Collision Integrals $\Omega_{p,q}^{l,s}$

The collision integrals are given by the general expression

$$\Omega_{pq}^{(l,s)} = \sqrt{\frac{kT}{2\pi m_{pq}}} \int_0^\infty e^{-\gamma_{pq}^2} \gamma_{pq}^{2s+3} Q^{(l)}(g_{pq}) \, d\gamma_{pq}$$ (39)

Here $\gamma_{pq} = \left(m_{pq} g_{pq}^2 / 2kT \right)^{1/2}$, g_{pq} is the initial relative speed of the colliding molecules, and $Q^{(l)}$ is the total collision cross section,

$$Q^{(l)} = 2\pi \int_0^\infty \left(1 - \cos^l \chi \right) b \, db \tag{40}$$

χ is the deflection angle,

$$\chi (g, b) = \pi - 2b \int_{r_m}^\infty \left(1 - \frac{b^2}{r^2} - \frac{\varphi (r)}{\frac{1}{2} m_{pq} g_{pq}^2} \right)^{-1/2} \frac{dr}{r^2} \tag{41}$$

$\varphi(r)$ is the interaction potential, and b, the impact parameter, is the distance of closest approach in the absence of the potential $\varphi(r)$. r_m is the positive root of the equation,

$$\frac{1}{2} m_{pq} g_{pq}^2 r^2 - r^2 \varphi(r) - \frac{1}{2} m_{pq} g_{pq}^2 b^2 = 0 \tag{42}$$

and m_{pq} is the reduced mass of the colliding molecules.

A2.1 Collision Integrals for the Intermolecular VSS Potential

The following expressions of the collision integrals $\boldsymbol{\Omega}_{p,q}^{l,s}$ for the VSS model hold for mixtures as well as for pure gases. They were calculated with "Mathematica" software and they are given by

$$
\boldsymbol{\Omega}_{pq}^{(1,1)} = - \left(\sqrt{\frac{\pi}{2}} \left(d_{\text{ref } p} + d_{\text{ref } q} \right)^2 m_p^3 \sqrt{\frac{kT \left(m_p + m_q \right)}{m_p m_q}} \right.
$$

$$
\times \left(\frac{m_p m_q}{kT \left(m_p + m_q \right)} \right)^{\frac{1}{2}(-7+\omega_p+\omega_q)} m_q^3 \left(\frac{kT_{\text{ref } pq} \left(m_p + m_q \right)}{m_p m_q} \right)^{\frac{1}{2}(-1+\omega_p+\omega_q)}
$$

$$
\left. \times \left(-5 + \omega_p + \omega_q \right) \right) \times \left(8k^3 T^3 \left(m_p + m_q \right)^3 \left(1 + \alpha_{pq} \right) \right)^{-1} \tag{43}
$$

$$
\boldsymbol{\Omega}_{pq}^{(2,2)} = \left(\sqrt{\frac{\pi}{2}} \left(d_{\text{ref } p} + d_{\text{ref } q} \right)^2 m_p^4 \sqrt{\frac{kT \left(m_p + m_q \right)}{m_p m_q}} \left(\frac{m_p m_q}{kT \left(m_p + m_q \right)} \right)^{\frac{1}{2}(-9+\omega_p+\omega_q)} \right.
$$

$$
\times m_q^4 \left(\frac{kT_{\text{ref } pq} \left(m_p + m_q \right)}{m_p m_q} \right)^{\frac{1}{2}(-1+\omega_p+\omega_q)}
$$

$$\times \alpha_{pq} \left(-5+\omega_p+\omega_q\right) \left(-7+\omega_p+\omega_q\right) \Bigg)$$

$$\times \left(8k^4 T^4 \left(m_p+m_q\right)^4 \left(1+\alpha_{pq}\right) \left(2+\alpha_{pq}\right)\right)^{-1} \tag{44}$$

$$\Omega_{pq}^{(1,2)} = \left(\sqrt{\frac{\pi}{2}} \left(d_{\text{ref } p}+d_{\text{ref } q}\right)^2 m_p^4 \sqrt{\frac{kT\left(m_p+m_q\right)}{m_p m_q}} \left(\frac{m_p m_q}{kT\left(m_p+m_q\right)}\right)^{\frac{1}{2}\left(-9+\omega_p+\omega_q\right)} \right.$$

$$\times m_q^4 \left(\frac{kT_{\text{ref } pq}\left(m_p+m_q\right)}{m_p m_q}\right)^{\frac{1}{2}\left(-1+\omega_p+\omega_q\right)}$$

$$\left. \times \alpha_{pq} \left(-5+\omega_p+\omega_q\right) \left(-7+\omega_p+\omega_q\right) \right)$$

$$\times \left(8k^4 T^4 \left(m_p+m_q\right)^4 \left(1+\alpha_{pq}\right) \left(2+\alpha_{pq}\right)\right)^{-1} \tag{45}$$

$$\Omega_{pq}^{(1,3)} = \left(\sqrt{\frac{\pi}{2}} \left(d_{\text{ref } p}+d_{\text{ref } q}\right)^2 m_p^5 \sqrt{\frac{kT\left(m_p+m_q\right)}{m_p m_q}} \right.$$

$$\times \left(\frac{m_p m_q}{kT\left(m_p+m_q\right)}\right)^{\frac{1}{2}\left(-11+\omega_p+\omega_q\right)} m_q^5 \left(\frac{kT_{\text{ref } pq}\left(m_p+m_q\right)}{m_p m_q}\right)^{\frac{1}{2}\left(-1+\omega_p+\omega_q\right)}$$

$$\left. \times \left(-5+\omega_p+\omega_q\right) \left(-7+\omega_p+\omega_q\right) \left(-9+\omega_p+\omega_q\right) \right)$$

$$\times \left(32k^5 T^5 \left(m_p+m_q\right)^5 \left(1+\alpha_{pq}\right)\right)^{-1} \tag{46}$$

A2.2 Collision Integrals for the Intermolecular VHS Potential

For the VHS model the collision integrals are the same as in the VSS model except that α_{pq} is set to 1.

References

1. M.N. Kogan, *Rarefied Gas Dynamics* (Plenum Press, New-York, 1969)
2. R.M. Velasco, F.J. Uribe, Physica A **134**, 339 (1986)
3. E.P. Gross, E.A. Jackson, Phys. Fluids **2**, 432 (1959)
4. S. Chapman, T.G. Cowling, *The Mathematical Theory of Non-Uniform Gases*, 3rd edn. (Cambridge University Press, Cambridge, 1970)
5. R. Brun, *Transport et Relaxation dans les Ecoulements Gazeux* (Masson, Paris, 1986)
6. J.O. Hirschfelder, C.F. Curtiss, R.B. Bird, *Molecular Theory of Gases and Liquids* (Wiley, New York, 1964)

7. F.R.W. McCourt, J.J.M. Beenakker, W.E. Kohler, I. Kuscer, *Nonequilibrium Phenomena in Polyatomic Gases*, vol. 1 (Oxford Science Publications, Oxford, 1990)
8. E.A. Mason, L. Monchick, J. Chem. Phys. **36**, 1622 (1962)
9. L. Monchick, K.S. Yun, E.A. Mason, J. Chem. Phys. **39**, 654 (1963)
10. P.C. Philippi, R. Brun, Physica A **105**, 147 (1981)
11. L. Monchick, A.N.G. Pereira, E.A. Mason, J. Chem. Phys. **42**, 3241 (1965)
12. K. Koura, H. Matsumoto, Phys. Fluids A **3**, 2459 (1991)
13. K. Koura, H. Matsumoto, Phys. Fluids A **4**, 1083 (1992)
14. J.G. Parker, Phys. Fluids **2**, 449 (1959)
15. J.D. Lambert, *Vibrational and Rotational Relaxation in Gases* (Clarendon, Oxford, 1977)
16. D.R. Millikan, R.C. White, J. Chem. Phys. **39**, 3209 (1963)
17. G.A. Bird, *Molecular Gas Dynamics and the Direct Simulation of Gas Flows* (Clarendon Press, Oxford, 1994)
18. C. Borgnakke, P.S. Larsen, J. Comp. Phys. **18**, 405 (1975)
19. S. Bock, E. Bich, E. Vogel, A.S. Dickinson, V. Vesovic, J. Chem. Phys. **120**, 7987 (2004)
20. S. Pascal, R. Brun, Phys. Rev. E **47**, 3251 (1993)
21. G.A. Bird, in *Rarefied Gas Dynamics*, ed. by S.S.Fisher (Progress in Astronautics and Aeronautics, AIAA, New York, 1981), pp. 239–255